

# SELF-SENSING MICROPUMP WITH GAS BUBBLE DETECTION FOR IMPROVED DOSING RELIABILITY

Kristjan Axelsson<sup>1\*</sup>, Mohammad Sheikhsarraf<sup>1</sup>, Phillip Höllein<sup>2</sup>, Dirk Lewke<sup>2</sup>, Martin Richter<sup>1</sup>

<sup>1</sup>*Fraunhofer EMFT, Hansastr. 27d, 80686 München*

<sup>2</sup>*RAPA Healthcare GmbH & Co. KG, Albert-Pausch-Ring 1, 95100 Selb*

\* Corresponding author: Tel.: +49 89 54759-454; E-mail address: kristjan.axelsson@emft.fraunhofer.de

---

## ABSTRACT

In micro-dosing system gas bubbles are a common source of dosing errors, by adding sensors to detect these the complexity and costs of the system increases. This paper introduces a novel approach for piezoelectric micropumps to detect gas bubbles without the usage of additional sensors like pressure or medium sensors. The proposed approach uses artificial intelligence (AI) methods directly implemented onto the micropump's high voltage driver circuit. The AI-methods are trained on a dedicated testbench, demonstrating successful gas bubble detection without increasing system costs and complexity and without the usage of additional sensors. This technology enhances dosing accuracy to ensure safer and more reliable micro-dosing applications.

**Keywords:** Piezoelectric, Micropump, Drug-Dosing, Self-Sensing, Artificial Intelligence, Gas-Bubble Detection

---

## 1. INTRODUCTION

In medical technology, biotechnology and the chemical industry, very small quantities of liquid often have to be precisely dosed. Micropumps can be used for this purpose [1]. To ensure high dosing accuracy and reliability, it is important to monitor possible faults and failures. In micro-dispensing technology, small gas bubbles are one of the main disturbances which are unavoidable in practical operation. This failure can lead to dosing errors or even risk the safety of patients during medication dosing if the required amount of medication is not dosed correctly [2]. There are various options for monitoring the dosing and detecting malfunctions and anomalies, such as gas bubble detection. However, these require additional external sensors, which makes the dosing system more complex and expensive. This paper introduces a new technique for detecting gas bubbles in micropump applications through a novel approach called **Self-Sensing**.

### 1.1. Piezoelectric diaphragm micropumps

The RAPA micropump is made up of thin stainless steel foils that are structured by etching and bonded using laser welding. Two of these foils contain the passive check valves and are welded on top of a ground plate. A piezoelectric diaphragm is then mounted on top of the stack. The diaphragm consists of a stainless steel foil with a zirconate titanate piezoelectric ceramic (PZT) glued on top (Figure 1).

To achieve a high compression ratio, a patented process called pre-tension (Patentnr. US9410641B2, 2016) is used [3]. This method bends the piezoelectric diaphragm into an upward position, creating the pump chamber. The micropump is then integrated into a microfluidic system, providing both

electrical and fluidic contacts. To actuate the piezoelectric micropump a rectangular voltage is applied. The voltage level is determined by the thickness of the piezoelectric material. During each stroke, one passive check-valve opens while the other one closes. Due to continuous repetition, this results in a constant volume transport through the pump chamber from the inlet to the outlet valve.

The experiments in this publication were carried out at Fraunhofer EMFT using 6 piezoelectric micropumps manufactured by RAPA.

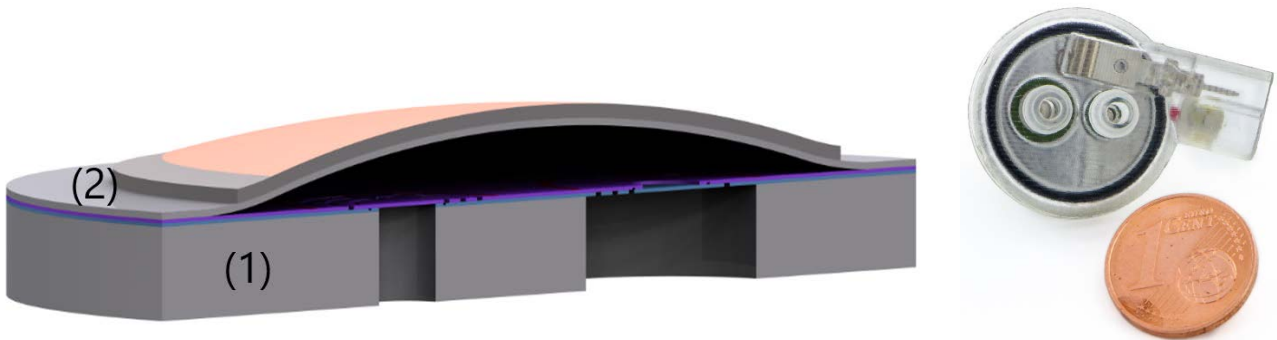


**Figure 1:** RAPA micropump made up of stacked steel foils with passive check valves (blue and purple layers) bonded by laser welding onto the base plate (1). The actuation is realized by a piezoelectric ceramic glued on top steel foil (2).

## 1.2. Self-Sensing theory

Piezoelectric actuators use the indirect piezoelectric effect to create mechanical deflection through an electrical control signal. In contrast, piezoelectric sensors use the direct piezoelectric effect to generate an electrical signal from mechanical deformation. The Fraunhofer EMFT intelligent pump utilizes both the indirect piezoelectric effect (actuator) and the direct piezoelectric effect (sensor) to achieve the desired self-sensing effect (Figure 2).

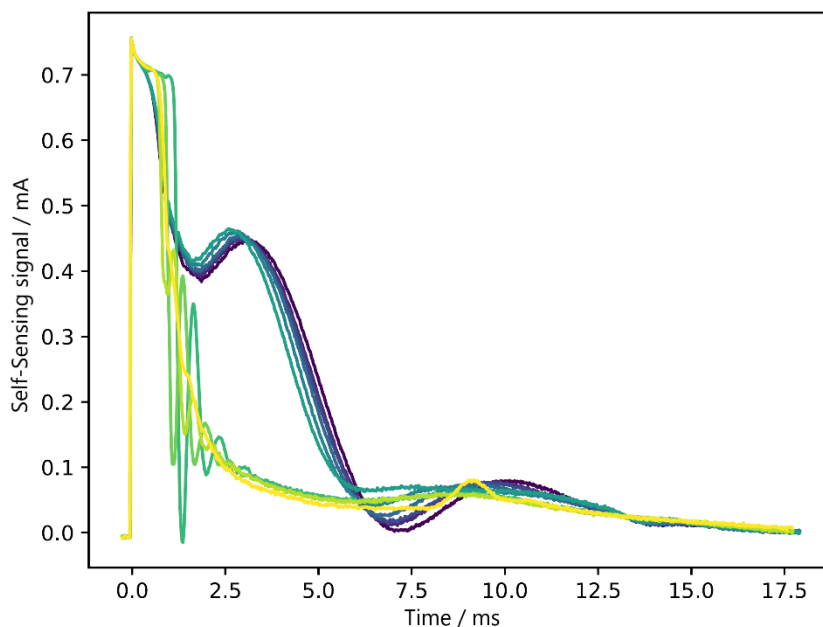


**Figure 2:** Self-Sensing signal measured with a current-to-voltage-converter amplifier circuit. Blue and dark green curves indicating a normal operation by pumping water. Yellow and light green signals indicating a gas bubble inside the pump chamber.

The Self-Sensing mechanism of piezoelectric micropumps relies on the indirect piezoelectric effect, which causes volumetric displacement in response to pressure  $p$ , voltage  $U$ , and the piezoelectric coupling factor  $C_E^*$ . The coupling factor is also dependent on the applied voltage  $U$ . Additionally, the fluidic capacity is denoted by  $C_p$ .

$$V(p, U) = C_p p + C_E^* U \quad (1)$$

The equation for the charge with electrical capacitance  $C_{el}$  follows the electrical analogy of fluidics.

$$Q(p, U) = C_{el} U + C_E^* p \quad (2)$$

Equation (2) represents the direct piezoelectric effect. To obtain the current  $I$ , we differentiate with respect to time, resulting in a four-term equation.

$$I(p, U) = C_{el} \frac{dU}{dt} + U \frac{dC_{el}}{dt} + p \frac{dC_E^*}{dt} + C_E^* \frac{dp}{dt} \quad (3)$$

The charging current of a constant capacitance is described by the first summand. The second summand describes the current resulting from the change in capacitance due to the big signal piezoelectric effect. The third term also describes a large signal effect, namely the change in the  $d_{31}$  coefficient at high voltages. The fourth summand describes the signal of interest, which is caused by the direct piezoelectric effect resulting from pressure changes in the pump chamber. Modulation of the charging current occurs when a bubble passes through the pump chamber, caused by a change in viscosity of the medium. Fore- and backpressure changes also affect pressure equalisation in the chamber and therefore the modulation of the loading current by the Self-Sensing signal.

### 1.3. Idea of a self-sensing micropump

Due to the fluid-mechanical couplings (see section 1.2) of the system, the sensor current modulates the charging current in a variety of ways so that various system states create a characteristic "fingerprint" in the "Self-Sensing" signal. To obtain this additional information, the self-sensing signal is measured by a load-free amplifier circuit.

Due to the high variability of environmental changes and their influence on the self-sensing signal, classical solutions cannot reliably distinguish between them. Artificial Intelligence methods (AI-methods) are therefore used to classify them. For example, by looking at the mean value of the current, some fault conditions, such as bubbles in the pump chamber or changes in back pressure, look the same.

The AI-methods are directly integrated onto the driver circuit of the piezoelectric diaphragm pump. This minimizes the increase in the circuit's footprint and eliminates the need for additional pressure and air bubble sensors, resulting in reduced system costs.

For an application-orientated use of the self-sensing property, the AI-methods are trained with suitable measurement data. This training data is generated at a measuring station specially developed for this purpose at Fraunhofer EMFT (section 2). This allows to generate various error states, such as a change in viscosity, gas bubbles, changes in system pressures, blockages of the fluidic channels. These so generated error scenarios can be clearly assigned to the measured Self-Sensing signal. The AI-methods are trained with the data obtained in this way on a high-performance computer and optimized for runtime and memory usage on Arm Cortex-M4 microcontrollers. The original driver

circuit of the micropump is enhanced with these AI-methods and is therefore able to recognize complex system states and react accordingly. Thanks to RAPA's controlled production process, the variance of the pumps is so low that an AI-method generated for one pump can also be used for others of the same generation design.

Training AI methods and deploying them on microcontrollers has become easier due to the availability of open-source libraries such as TensorFlow, TensorFlowLite, and CubeAI. However, obtaining appropriate training data for a specific problem remains a challenge. To address this, a novel testbench for micropumps was designed and implemented.

## 2. SELF-SENSING TESTBENCH

To obtain high-quality training data for various environmental scenarios, a suitable testbench was designed and implemented (Figure 3). This testbench generates basic operating conditions and specific failure scenarios, and the corresponding Self-Sensing signal is sampled.

Multiple controllers are required to set the desired environmental scenarios, such as inserting gas bubbles and changing system pressures. The piezoelectric micropump is actuated using a high-voltage signal driver. Pressure controllers and active valves are used to set different pressure levels at the inlet and outlet of the fluidic system. To record these generated operating states and the corresponding self-sensing signal, various types of sensors are required, such as gas bubble detectors and pressure sensors. This information is collected and later used to label the training data.

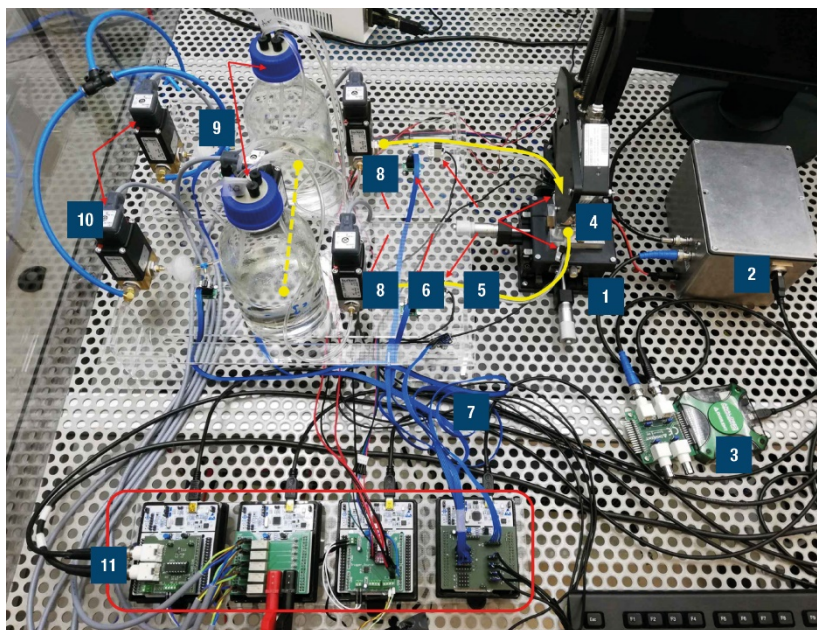


**Figure 3:** 1) Piezoelectric diaphragm pump 2) Self-Sensing circuit 3) Oscilloscope to measure Self-Sensing signal 4) Optical deflection sensor to measure diaphragm movement 5) Gas-bubble detectors 6) Pressure sensors 7) Temperature sensor 8) 3/2 valve to change medium from water to air 9) Inlet and outlet-reservoir 10) 3/2 valve to connect pressure controller with inlet or outlet 11) Electronics to control sensors and actuators of the testbench. Below the testbench: Function generator, Piezo-Driver, Pressure controller.

A 3/2-valve is used at the inlet reservoir to switch the medium in the system between water and air. The valve allows a controlled insertion of gas bubbles of varying sizes into the fluidic periphery by regulating the switching time of the valve at the inlet tubing. Additionally, a 2/2 valve is installed between the input and output reservoirs to enable water to flow back from the outlet reservoir to the inlet reservoir (refer to the yellow dashed line in Figure 3). The next step involves generating various pressure scenarios by setting the inlet and outlet pressure using a pressure controller.

After the generation of the desired error states follows the detection of the corresponding environmental configurations and sampling the Self-Sensing signal. Four gas bubble sensors are used to detect bubbles: The gas bubble is detected by the first sensor as it enters the inlet tubing. The second sensor detects the bubble as it enters the pump inlet. The third sensor detects the bubble as it exits the pump chamber, and the fourth sensor detects the bubble as it leaves the system. To measure the applied pressure, four sensors are utilized: One for the inlet reservoir, one for the outlet reservoir, and one each for the pump inlet and outlet.

Finally, the self-sensing signal is sampled by the self-sensing electronic. All this data is later used for training and labelling with the obtained sensor data.

To train an AI-method to detect gas bubbles inside the piezoelectric micropump a suitable dataset for 6 devices was generated. To realize this the fluidic system is filled with water and gas bubbles are inserted. The measurement takes 5 minutes at a pump frequency of 25 Hz, resulting in 7500 pump strokes. The number of pump strokes with gas bubbles inside the pump chamber ranges from 1000 to 3000 cycles.

### 3. AI-METHODS FOR GAS BUBBLE DETECTION

Models are trained and evaluated on the PC with the usage of Cube-AI to estimate the Flash usage and runtime on the Arm Cortex-M4 microcontroller. In this work we compare different types of AI-methods such as Random Forest, Deep Neural Networks (DNN) and Convolutional Neural Networks (CNN).

In binary classification problems with imbalanced classes caused by rare events, the F1-score metric is crucial. The F1 score (equation 4) is the harmonic mean of precision and recall, with a best value of 1 and a worse value of 0. F1-score is the classification metric in this work to evaluate the accuracy of the AI-methods [5].

$$F1 - score = \frac{2 * Precision * Recall}{Precision + Recall} \quad (4)$$

The precision ratio represents the number of true positive results that were accurately predicted by the model.

$$Precision = \frac{TruePositive}{TruePositive + FalsePositive} \quad (5)$$

Recall, also known as sensitivity, is a metric that measures the model's ability to correctly identify positive results.

$$Recall = \frac{TruePositive}{TruePositive + FalseNegative} \quad (6)$$

As previously stated, AI training is conducted on a high-performance PC and then transferred to a Cortex-M4 microcontroller. However, a challenge with this approach is the varying implementations of AI model libraries. To address this, the Cube-AI from STMicroelectronics is utilized to directly compare AI methods using the same metric on a PC. The metrics used are memory usage in kilobytes and runtime in Multiply-Accumulate (MACC).

In this work gas bubble data was recorded for 6 micropumps and trained by procedure called cross evaluation. To obtain metrics for a single device, named as test-device, data for training and evaluation is generated from the remaining five devices. The F1-score is then calculated for each of the 6 micropumps and 50 different models (18 Random Forest, 16 Deep Neural Networks and 16 Convolutional Networks). This procedure is then repeated for each of the other 5 devices. The F1-score is shown in Figure 4. The memory usage in kilobytes and the runtime in MACC's for each of the 50 models is shown in Figure 5.

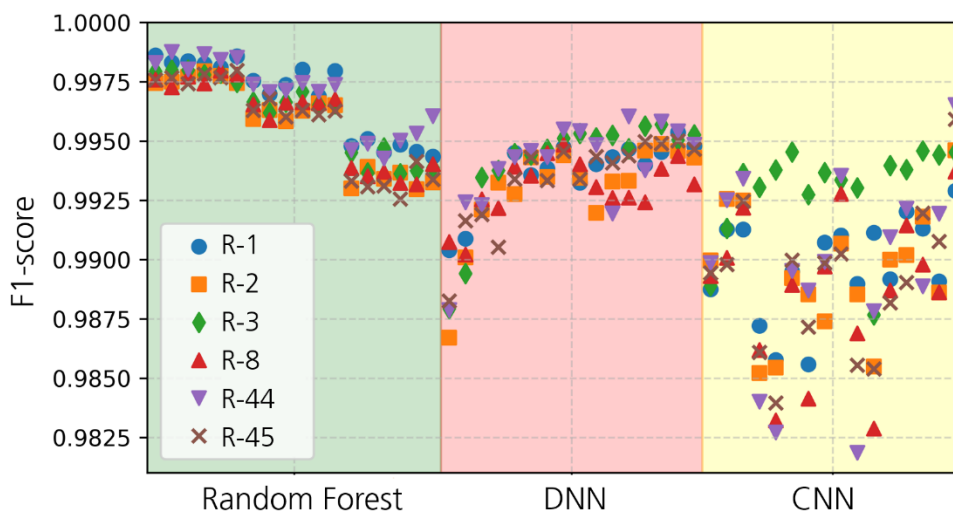


**Figure 4:** F1-score for Random Forest, Deep-Neural Networks and Convolutional Neural Networks. The Random Forest models shown the highest accuracy (F1-score).

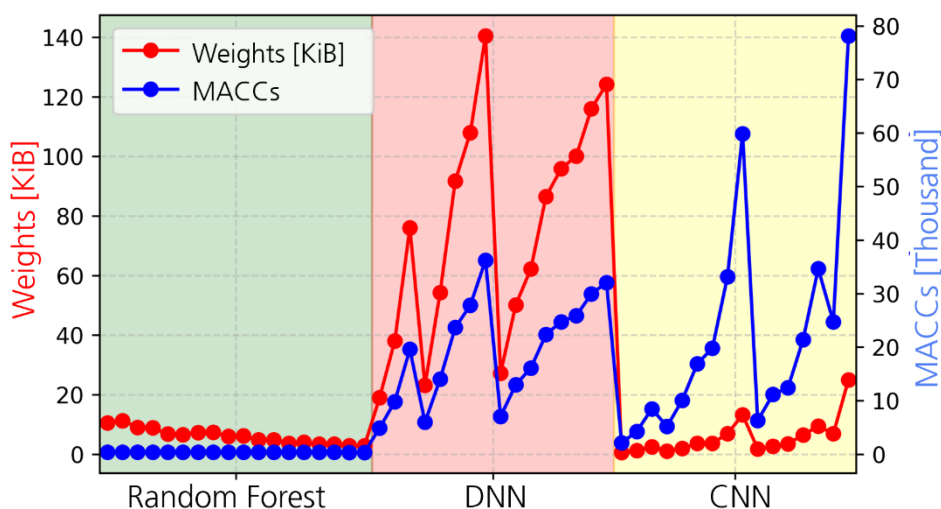


**Figure 5:** Flash consumption in kilobytes and runtime in MACC's for Random Forest, Deep-Neural Networks and Convolutional Neural Networks. The Random Forest models performs best by considering memory usage and execution time.

### 3.1. Results

This work demonstrates that AI methods can be used to detect gas bubbles within the pump chamber by analysing the self-sensing signal. Therefore, no additional sensors are needed.

If a gas bubble is detected in the pump chamber, the number of pump strokes can be counted. By multiplying the number of strokes with air by the stroke volume of the micropump, the size of the gas bubble can be estimated. This can be achieved with a small increase in the electronics footprint and a software update to the standard microcontroller for high voltage generation.

This new technology improves the micropump's functionality at a similar cost and size, representing a significant advancement in the safety and reliability of micro-dosing applications.

## 4. CONCLUSION AND OUTLOOK

This novel use of the sensory properties of the piezoelectric actuator enables the piezoelectric diaphragm pump to realize a self-monitoring feature for micro-dosing systems. This allows for observation of normal operation and detection of disturbances such as gas bubbles, without the need for additional sensors. This concept of gas bubble detection and quantification can improve dosing accuracy and precision in drug delivery applications by compensating for undosed volume caused by gas bubbles.

In addition to detecting and compensating for gas bubbles, a further stage of development is to detect and compensate for fluctuations in backpressure.

This concept enables real-time extraction of information from the piezoelectric actuator's regular actuation signal without the need for additional sensors. It demonstrates how the piezoelectric actuator interacts with its environment. As gas bubbles and backpressure fluctuations, including catheter occlusion, can interfere with drug dosing, this method has the potential to disrupt drug dosing with micropumps to a new level of efficiency, reliability and cost effectiveness.

## REFERENCES

- [1] A. Bußmann, H. Leistner, D. Zhou, M. Wackerle, Y. Congar, M. Richter and J. Hubbuch, "Piezoelectric Silicon Micropump for Drug Delivery Applications" Applied Science, 2021.
- [2] A. Bußmann, C. Durasiewicz, S. Kibler and C. Wald, „Piezoelectric titanium based microfluidic pump and valves for implantable medical applications,“ Sensors and Actuators, 2021.
- [3] M. Richter, M. Wackerle and M. Herz, „Method for manufacturing a bending transducer, a micro pump and a micro valve, micro pump and micro valve“. Patent US9410641B2, 2016.
- [4] D. Horsch „Untersuchung des struktur-, und fluidmechanischen Verhaltens einer piezoelektrischen angetriebenen Mikromembranpumpe“, München: TUM, 2009.
- [5] C. M. Bishop and N. M. Nasrabadi, Pattern recognition and machine learning. Springer, 2006, Vol. 4